Amorphization and magnetic properties of Co_2Ge during mechanical milling

G. F. Zhou and H. Bakker
Van der Waals–Zeeman Laboratorium, Universiteit van Amsterdam, Valckenierstraat 65, 1018 XE Amsterdam, The Netherlands
(Received 17 May 1993; revised manuscript received 20 September 1993)

The structural features and magnetic properties of the intermetallic compounds α-Co_2Ge (low-temperature phase, LTP) and β-Co_2Ge (high-temperature phase, HTP) upon mechanical milling were investigated by x-ray diffraction, differential scanning calorimetry (DSC), and magnetic measurements. It turns out that starting from both the ordered LTP with Co_2Si-type orthorhombic structure and the ordered HTP with Ni_2In-type hexagonal structure mechanical milling generates atomic disorder during the early stage of milling and transforms the materials to an amorphous state after long-time milling. Both the LTP and the HTP are ferromagnetic at lower temperatures with Curie temperatures of 46.4 K and 6 K, respectively. The magnetic moment per Co atom at 4.2 K is $0.113\mu_B$ in the LTP and $0.103\mu_B$ in the HTP. The average magnetization at 4.2 K and the Curie temperatures of the LTP and the HTP continuously increase with increasing milling time in the early stage of milling. During the intermediate stage of milling, a discontinuous decrease in magnetic-ordering temperature (a mixture of two magnetic phases) is observed in the LTP, which strongly indicates the formation of the amorphous phase. In DSC scans the exothermic heat effects are evident, which correspond to the atomic reordering process of the disordered compounds and to the crystallization of the amorphous phase and the subsequent growth of nanometer-scale crystallites. All physical parameters measured in the present investigation tend to become constant after prolonged periods of milling. The good agremeent of all the experimental results obtained by different techniques proves that by mechanical milling well-defined metastable states in Co_2Ge are generated. The amorphous phase as the final state shows spin-glass behavior: a transition at 43 K from the paramagnetic state to the spin-glass state is clearly observed upon cooling from room temperature to liquid-helium temperature.

I. INTRODUCTION

An intermetallic compound may transform to an amorphous phase[1–4] or to a disordered solid solution[5,6] at room temperature under continuous mechanical impact in a high-energy ball mill. In some systems, for instance in Ni_3Sn_2 and Co_3Sn_2, mechanically induced phase transformations from a complex crystal structure to a somewhat simpler crystal structure, which exists in phase diagram at higher temperatures, have also been found.[7,8] It was accompanied by the creation of atomic disorder of the type "redistribution of 'interstitials' over two different types of lattice sites." The materials did not transform to the amorphous state even after prolonged periods of milling. In the present investigation, we have chosen the intermetallic compound α-Co_2Ge for ball milling in the same mill as was used in Refs. 7 and 8. In the phase diagram[9] the intermetallic compound Co_2Ge is very similar to Ni_3Sn_2 and Co_3Sn_2. That is, the compound Co_2Ge crystallizes in an orthorhombic structure at room temperature with a homogeneity range from 59 to 68 at. % Co. It exists in the low-temperature phase (LTP) α-Co_2Ge up to a temperature of 625 °C depending on composition. Above 625 °C the compound transforms to a high-temperature phase (HTP) β-Co_2Ge with a hexagonal crystalline structure, which melts at much higher temperatures. The aim of this study is to assess whether atomic disorder can also be introduced in the LTP by mechanical milling and whether the LTP transforms to the HTP after long milling time, and whether the material finally transforms to an amorphous state. For comparison, mechanical milling has also been performed on the HTP. The process of mechanical milling was monitored by x-ray diffraction, differential scanning calorimetry (DSC), high-field and low-field magnetization measurements, and ac magnetic susceptibility measurements.

II. EXPERIMENTAL DETAILS

The intermetallic compound α-Co_2Ge (LTP) was obtained by arc melting of weighed amounts of pure cobalt and germanium in a purified argon atmosphere. Arc melting was repeated several times in order to obtain a homogeneous sample. The arc-melted button was crushed to powder and annealed at 500 °C for 2 h and at 450 °C for 24 h, and subsequently annealed at 400 °C for 100 h. The x-ray-diffraction pattern of the annealed sample shows the characteristics of the low-temperature phase with an orthorhombic structure.

The compound Co_2Ge for the quenching experiment was obtained in the same way as described above. Rapid quenching of the Co_2Ge from 800 °C was performed in a special powder quenching device[10] (LOPOQ) to obtain the HTP. The melt-spinning technique was used to quench the Co_2Ge compound from the liquid state to room temperature. The cooling rate was about 10^7 K per sec.

Mechanical milling was carried out in a hardened steel vacuum vial (inner diameter 6.5 cm) with a tungsten carbide bottom. Inside the vial, a hardened steel ball with a

diameter of 6 cm was kept in motion by a vibrating frame (Fritsch: Pulverisette 0), upon which the vial was mounted. In order to prevent reactions with oxygen or nitrogen, the milling was performed under continuous pumping. During the milling the vacuum was kept at a level of about 10^{-6} Torr. The starting amount of material was four grams. X-ray-diffraction powders were taken from the samples milled for different periods and after the x-ray-diffraction experiment the powder was used for ac magnetic susceptibility and magnetization measurements, and subsequently for DSC analyses.

X-ray-diffraction patterns were taken at room temperature by means of a Philips diffractometer with vertical goniometer using Cu $K\alpha$ radiation. The high-field magnetization measurements at 4.2 and at 77 K were performed in the Amsterdam High-Field Installation[11] in which magnetic fields up to 40 T can be generated in a semicontinuous way. A stepwise field profile up to 21 T was used. The sensitivity of this magnetometer is about 10^{-5} Am^2. The ac magnetic susceptibility measurements have been carried out from room temperature to liquid-helium temperature in self-constructed equipment. The low-field magnetization was measured in a self-designed magnetometer. The sensitivity of the magnetometer is better than 10^{-5} Am^2. Differential scanning calorimetry (DSC) measurements were carried out in a Perkin-Elmer DSC-7 in argon gas flux at a speed of 30 cc/min to protect the sample against oxidation. A heating rate of 10 K/min was used in the DSC scans. The scan was repeated twice for each sample. The temperature and the reaction heat were calibrated by pure indium and zinc standards.

III. EXPERIMENTAL RESULTS

A. Orthorhombic α-Co_2Ge (LTP)

1. Structure and thermal stability

Figures 1 and 2 show the x-ray diffraction patterns of the LTP after various periods of milling as well as the compound quenched from 800 °C (the top pattern in Fig. 2 marked as HTP). The pattern of the as-prepared material (0 h) is identified as the low-temperature phase α-Co_2Ge (LTP) having the Co_2Si-type orthorhombic structure with space group *Pnma*. This is in agreement with literature.[12] The pattern of the quenched sample (marked as HTP in Fig. 2) is characteristic of the high-temperature phase β-Co_2Ge (HTP), the Ni_2In-type hexagonal structure with space group $P6_3/mmc$. The orthorhombic structure of the LTP is distinguished from the hexagonal structure of the HTP by some extra reflections which appear in the x-ray diffractograms of the sample in the low-temperature phase. It is clearly seen that during mechanical milling the intensity of the x-ray-diffraction patterns of the LTP decreases gradually and all peaks become broader with increasing milling time. After 20 h of milling, some Bragg peaks of the LTP disappear and the other peaks become much broader than in the starting compound (0 h). After 40 h of milling, many peaks of the LTP disappear and the peaks around $2\theta=45°$ are difficult to separate. After 60 h of milling most of the Bragg peaks of the LTP disappear and the peaks around $2\theta=45°$ become two overlapping broad peaks. This indicates that the LTP is completely disordered after 60 h of milling. After 80 h of milling the two overlapping broad peaks around $2\theta=45°$ become one rather broad peak and the intensity of the other peaks decreases, which implies that the material starts amorphization. After 120 h of milling almost all the Bragg peaks disappear except for the rather broad peak at $2\theta=45°$, which means that the majority of the material is transformed to the amorphous

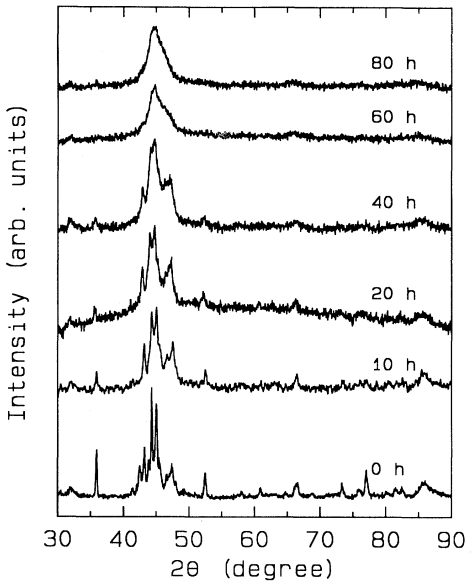

FIG. 1. X-ray-diffraction patterns of the LTP after various periods milling up to 80 h.

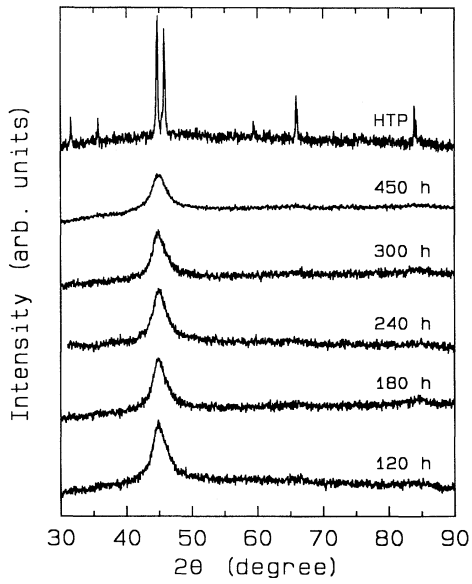

FIG. 2. X-ray diffraction patterns of the LTP after milling periods longer than 80 h as well as the HTP obtained by quenching from 800 °C.

state. After 180 h of milling all peaks disappear except for the broad halo at $2\theta=45°$. This means that the phase transformation of the crystalline to an amorphous state is completed after 180 h of milling. Upon further milling no change in x-ray-diffraction patterns can be observed. This implies that there is no structural change in the late stage of milling but that the material in fact is becoming more and more homogeneous. This is confirmed by the change of the sharpness of the pronounced cusp in magnetic susceptibility measurements which will be discussed later (see Fig. 10). Apparently, a phase transformation from the LTP to the HTP such as in Ni_3Sn_2 (Ref. 7) and Co_3Sn_2 (Ref. 8) does not occur during ball milling.

The thermal stability of all the ball-milled samples is studied by differential scanning calorimetry (DSC) analyses. Figures 3 and 4 show the DSC scans of the LTP after various periods of milling. It can be seen that in the DSC scan of the starting compound (0 h) there is an endothermic peak at a temperature of 680 K, which corresponds to the equilibrium phase transition from the LTP to the HTP as is expected from the phase diagram. The heat of the phase transition is estimated as 1.81 kJ/mol. This endothermic peak also appears in ball-milled materials at somewhat lower temperature. The intensity of the endothermic peak decreases gradually with increasing milling time. Figure 5 shows the heat consumed in the endothermic transition as a function of milling time. It is clear that the heat involved in the endothermic transition continuously decreases with increasing milling time in the early stage of milling. After 80 h of milling it tends to become constant with a heat content of about 0.2 kJ/mol. An exothermic peak at a temperature of 550 K is evident in the DSC scan of the sample after 10 h of milling. The heat involved in the transition is about 0.3 kJ/mol. With increasing milling time this exothermic peak becomes more and more pronounced and becomes broader and broader. The heat content is increased to 2.4 kJ/mol after 40 h of milling and to about 3.3 kJ/mol after 60 and 80 h of milling. Another weak exothermic peak at about 430 K in the DSC scan of the sample milled for 20 h is detectable. After 40 h of milling, it becomes more pronounced with a heat content of 0.3 kJ/mol. After 80 h of milling the intensity of this peak becomes rather strong. After 180 h of milling, the intensity of this peak considerably increases. Upon further milling it tends to saturate. It should also be noted that starting from the sample milled for 120 h another exothermic peak is observed at 740 K. The peak tempera-

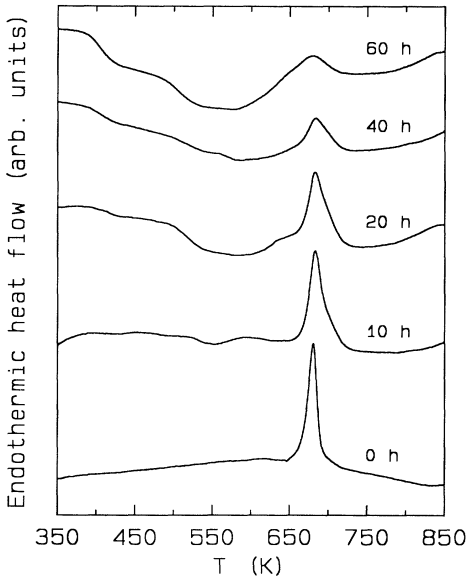

FIG. 3. DSC scans of the LTP after various periods milling up to 60 h.

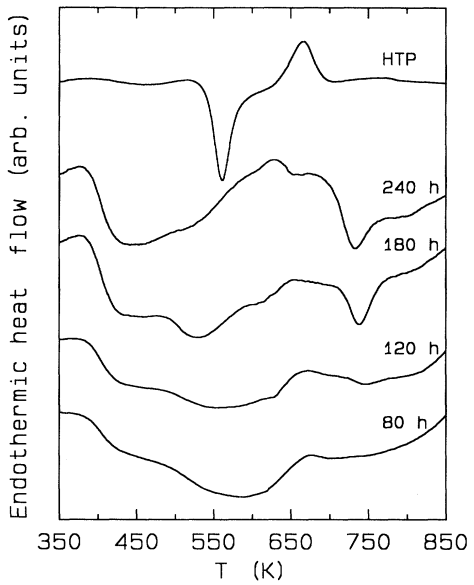

FIG. 4. DSC scans of the LTP after milling periods longer than 60 h as well as the HTP obtained by quenching from 800 °C.

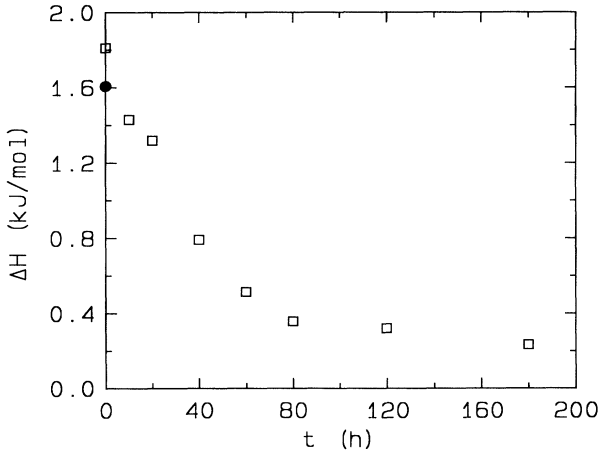

FIG. 5. Heat consumed in the endothermic transition occurring in the DSC scans in Figs. 3 and 4 as a function of milling time. The filled circle denotes the result on HTP after this material first transformed from HTP to LTP at lower temperatures.

ture shifts somewhat to lower temperature upon further milling and it becomes more pronounced. The heat involved in the exothermic transition is estimated as 0.8 kJ/mol and the peak temperature shifts to 730 K in the sample milled for 240 h. The DSC scan of the HTP quenched from 800 °C is also shown in Fig. 4 (the top curve marked as HTP). A very sharp exothermic peak at the temperature of 560 K is observed, which corresponds to the phase restoration of the metastable HTP to the LTP. Upon further heating, an endothermic peak at 670 K appears which indicates the equilibrium phase transition of the LTP to HTP like in the original LTP sample. The heat involved in the exothermic transition is estimated as 2.6 kJ/mol. The heat consumed in the endothermic transition is about 1.6 kJ/mol, which is lower than that in the LTP (1.8 kJ/mol) (see also Fig. 5).

For a better understanding of the heat effects, we heated the samples milled for 40 and 180 h in the DSC to various temperatures and rapidly cooled them down subsequently to room temperature. Figure 6 shows the x-ray-diffraction patterns of the sample milled for 180 h after heating to different temperatures. The curve indicated by 423 K, the peak temperature of the first exothermic transition, shows a number of extra reflections in comparison to the pattern of the ball-milled sample (see Fig. 2 the pattern of the LTP milled for 180 h). This indicates that the first exothermic peak corresponds to the crystallization of the amorphous phase. In fact, it is also partially resulting from the release of strains. This is confirmed by the observation of the first exothermic transition in the DSC scans of the samples after various periods of milling up to 60 h (the disordered crystalline samples), which is responsible for the release of strains. The pattern marked as 573 K, the end of the second exothermic peak, shows more extra reflections, which means that the second exothermic transition corresponds to the atomic ordering process. The fact that the first two exothermic transitions appearing in the DSC scan of the amorphous phase are too close to separate, makes it impossible to derive the heat for crystallization and subsequent atomic ordering separately. So we take the two exothermic transitions as one broad peak. The total heat content in the broad exothermic transition is then 4.2 kJ/mol in the temperature range from 380 to 580 K in the samples after 180 and 240 h of milling. The second exothermic transition in the DSC scans of the samples after milling up to 60 h corresponds to the atomic reordering process. This is judged by the observation of a great number of additional x-ray-diffraction peaks in the sample milled for 40 h after heating to the end of this transition. After further heating to 693 K, the end of the endothermic peak, the x-ray-diffraction pattern is characteristic of the LTP. In principle it should be that of the HTP. That the cooling rate in the DSC is not fast enough causes the formation of the LTP during cooling. After heating up to 773 K, the end of the third exothermic peak, the pattern is again characteristic of the LTP for the same reason. Comparing the pattern indicated by 773 K with that indicated by 693 K, it is observed that all the peaks resulting from the sample heated up to 773 K are much sharper than those of the sample heated to 693 K, which means that the third exothermic peak is responsible for the growth of the crystallites.

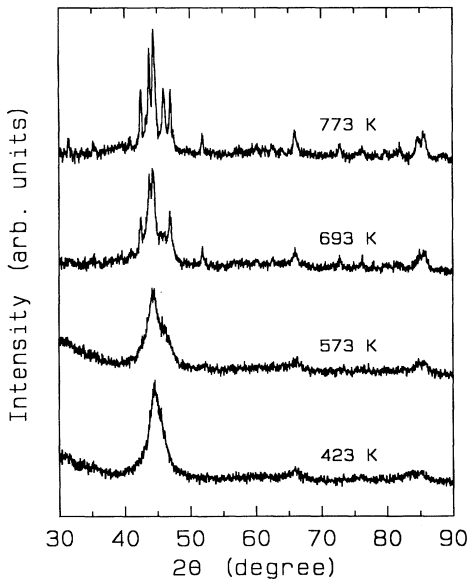

FIG. 6. X-ray-diffraction patterns of the LTP milled for 180 h after heating to different temperatures in DSC.

2. *Magnetic properties*

Typical magnetization curves at 4.2 K of the LTP after various periods of milling as well as the HTP quenched from 800 °C are shown in Fig. 7. The magnetization at 21 T for the samples milled for various periods is plotted in Fig. 8 as a function of milling time and tabulated in Table I. The filled circle denotes the magnetization of HTP. From Fig. 8 and Table I one can see that the magnetization of the LTP ($0.113\mu_B$/Co atom) is slightly larger than that of the HTP ($0.103\mu_B$/Co atom). The magnetization of LTP increases gradually with increasing milling time when the milling time is shorter than 80 h. After 80 h of

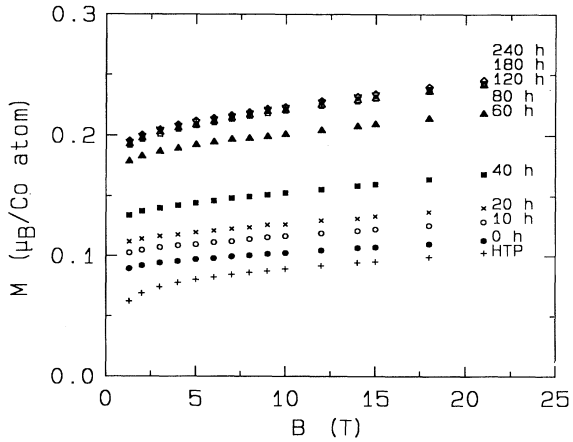

FIG. 7. Typical high-field magnetization curves at 4.2 K of the LTP after milling for various periods as well as the HTP obtained by quenching from 800 °C.

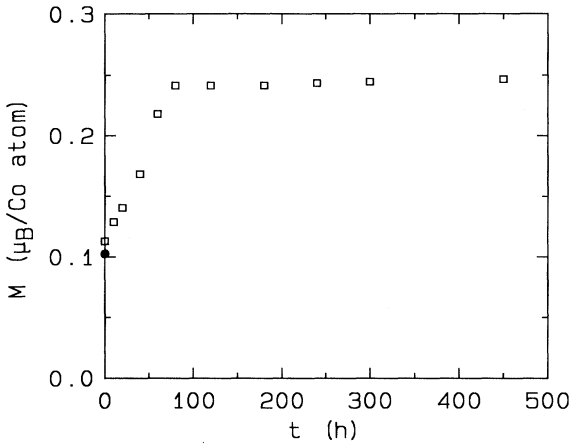

FIG. 8. Magnetization at 4.2 K of the LTP at 21 T as a function of milling time. The filled circle denotes the measurement on the HTP.

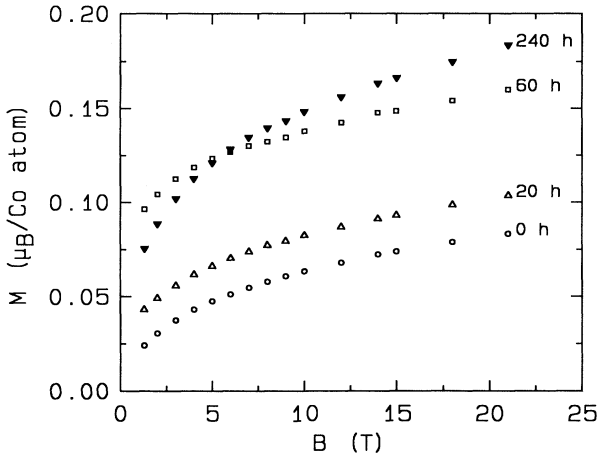

FIG. 9. Typical high-field magnetization curves at 77 K of the LTP after various periods of milling.

milling, it reaches a value of $0.241\mu_B$/Co atom. After further milling the magnetization is only slightly dependent on milling time. Moreover, the magnetization curves measured at 77 K for some typical samples are displayed in Fig. 9. The shape of the magnetization curves at 77 K of the samples milled for 0, 20, and 60 h is quite similar, but somewhat different for the sample milled for 240 h.

The magnetic-ordering temperatures of the LTP after various periods of milling and of the HTP were derived from the ac magnetic susceptibility vs temperature measurements. The measurement of magnetization vs external magnetic field at various temperatures was used to confirm the magnetic-ordering transitions. The temperature dependence of the real part of the ac susceptibility χ' of the LTP after various periods of milling, as well as the HTP quenched from 800 °C is shown in Fig. 10. From this figure, at least two aspects can be clearly noticed. First, an anomaly in the LTP (0 h) at 46.4 K and in the HTP at about 6 K is evident, which corresponds to the magnetic-ordering transition. Secondly, this anomaly is very sensitive to mechanical milling. When the milling time is shorter than 60 h, the transition temperature continuously increases with increasing milling time and the transition broadens. In some cases the transition in the real part of the ac susceptibility (χ') is not sharp. Therefore the transition temperatures were taken as the temperature where the imaginary part of the ac susceptibility (χ'') achieves a minimum. The thus obtained results are given in Table I (the third and/or the fourth column). After 60 h of milling the transition temperature reaches a maximum of about 84 K. After 80 h of milling another anomaly at about 40 K starts to appear, which corresponds to the magnetic-ordering transition of the amorphous phase. This indicates that the amorphization of the material starts at a milling time of 80 h. After 120 h of milling the anomaly at about 40 K becomes predominant, which means an increase of the amorphous fraction upon further milling. After 180 h of milling the anomaly at 84 K disappears and the anomaly at about 40

TABLE I. Magnetic moment M (μ_B/Co atom) at 4.2 K, ferromagnetic Curie temperature T_C (K) or freezing temperature T_f (K), and the phase status of the LTP upon ball milling. The results of the HTP quenched from 800 °C are also included.

Milling time (h)	M (μ_B/Co atom)	T_C (K)	T_f (K)	Phase status
0 (α-Co_2Ge LTP)	0.113	46.4		Ordered crystalline
10	0.129	48.5		Disordered crystalline
20	0.140	52.2		Disordered crystalline
40	0.168	65.5		Disordered crystalline
60	0.218	84.2		Disordered crystalline
80	0.241	84.1	40.3	Crystalline+amorphous
120	0.241	84.8	40.1	Crystalline+amorphous
180	0.241		40.2	Amorphous
240	0.243		43.1	Amorphous
300	0.245		43.4	Amorphous
450	0.247		43.8	Amorphous
β-Co_2Ge (HTP)	0.103	6		Ordered crystalline

K becomes a pronounced cusp. This means that the phase transformation from a crystalline to an amorphous state is completed after 180 h of milling. The sharp cusp in the ac susceptibility vs temperature curve indicates that the amorphous phase shows a spin-glass (SG) behavior. This will be discussed in more detail later. Upon further milling the cusp becomes sharper and sharper and the cusp temperature slightly increases. This means that the material is homogenized during the late stage of milling. The above observation is consistent with the x-ray diffraction and gives more detailed information about the process during the intermediate stage of milling.

Figure 11 shows the magnetization curves of the LTP after 0 and 240 h of milling measured at various temperatures and of the HTP. In Fig. 12 the results of the inverse initial susceptibility vs temperature are given for the LTP after 0, 60, and 240 h of milling and for the HTP. Due to the fact that the magnetization does not depend linearly on the applied field in the vicinity of the magnetic-ordering temperature, we were not able to measure initial susceptibility directly. The initial susceptibility was derived from the corresponding M^2 vs B/M plots (M = magnetic moment per Co atom), so-called Arrott plots, which are usually straight lines near the critical temperature. The inverse initial susceptibility is then

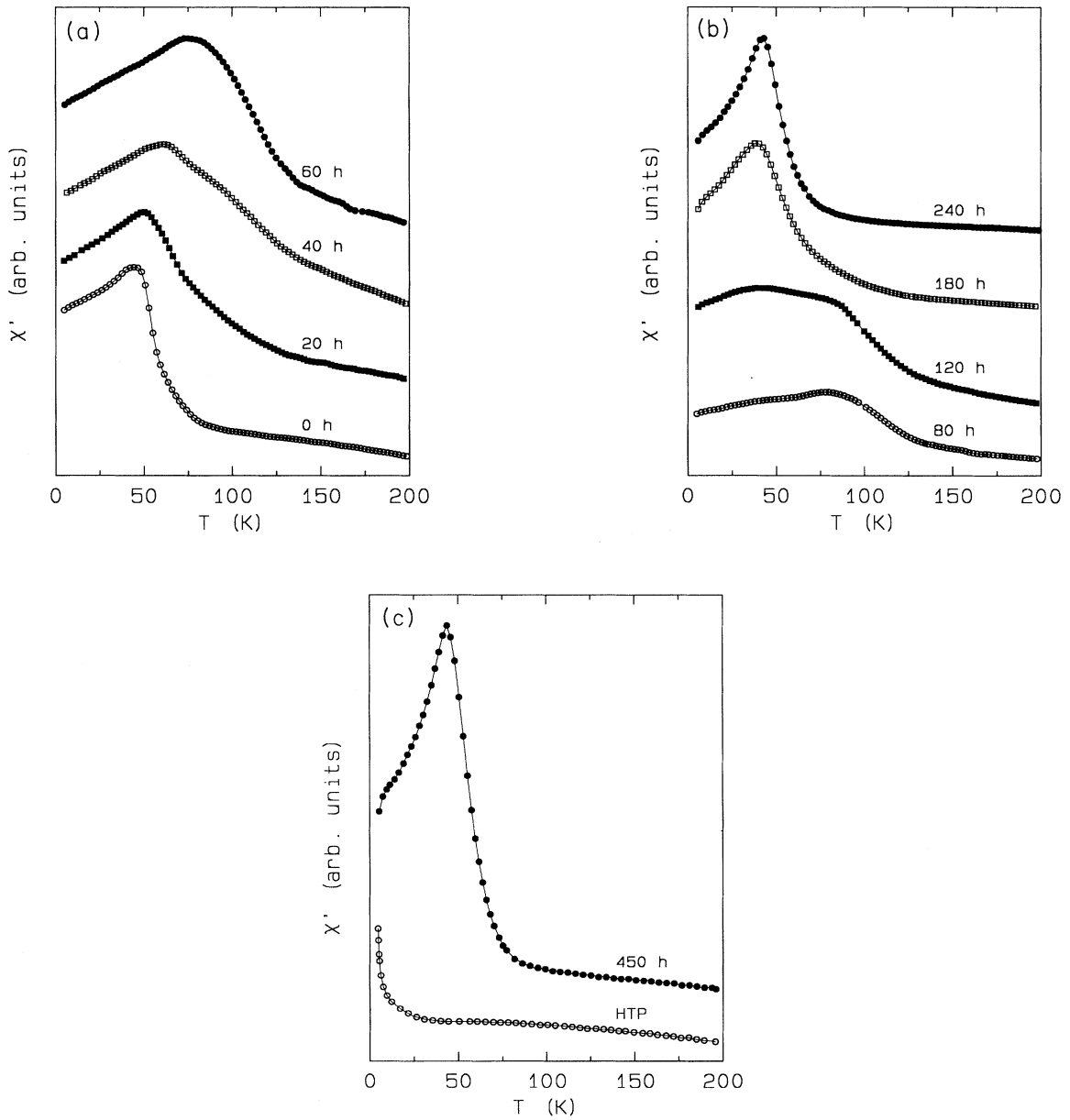

FIG. 10. Temperature dependence of the real part of the ac magnetic susceptibility χ' of the LTP after various periods of milling as well as the HTP in an external ac field of 0.06 mT. The frequency of 109 Hz was used during measuring.

given by the intercept of the straight line with the B/M axis. The paramagnetic susceptibility of these materials was analyzed in terms of the Curie-Weiss law:

$$\chi = \frac{C}{T-\Theta_p} , \quad (1)$$

where C is the Curie constant, $C = N_0 g^2 \mu_B^2 J(J+1)/3k_B$, and Θ_p is the paramagnetic Curie temperature. Here N_0 is the number of magnetic atoms per unit volume, J the angular momentum, μ_B the Bohr magneton, g and Landé factor, and k_B the Boltzmann constant. From Eq. (1), the temperature intercept of $1/\chi$ vs T gives the value of Θ_p, and the slope $1/\chi$ yields the effective magnetic moment per Co atom in Bohr magnetons p_{eff}:

$$p_{\text{eff}} = g[J(J+1)]^{1/2} = \left[\frac{3k}{N_0 \mu_B^2 d(1/\chi)/dT} \right]^{1/2} . \quad (2)$$

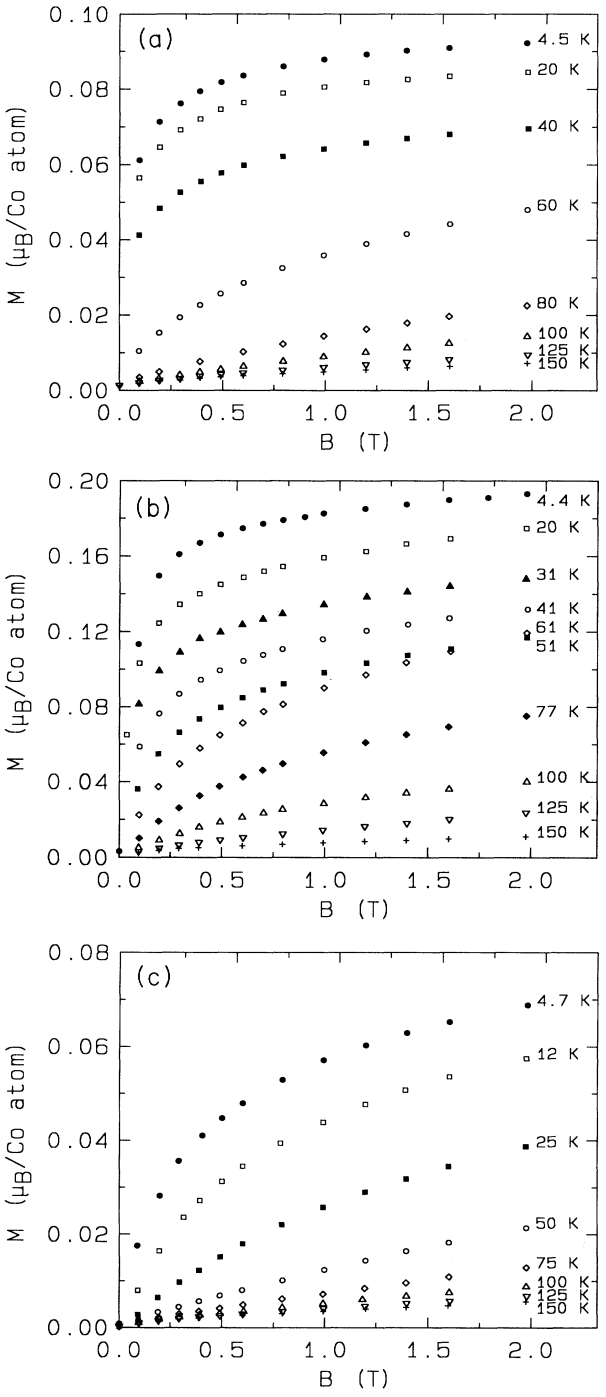

FIG. 11. Magnetization vs external magnetic fields of the LTP milled for (a) 0 h, (b) 240 h and the HTP (c) at various temperatures.

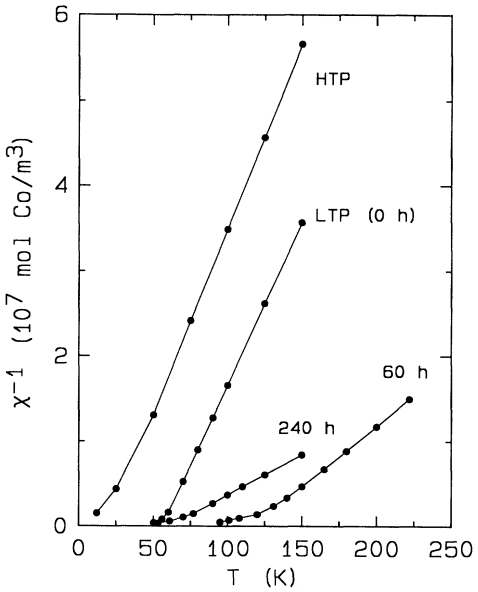

FIG. 12. Inverse susceptibility of the LTP after 0, 60, and 240 h of milling and the HTP as a function of temperature.

The thus obtained results are collected in Table II. It is clear that the paramagnetic Curie temperatures of the LTP after 0, 60, and 240 h of milling and of the HTP are positive, which means that the LTP after 0 and 60 h of milling and the HTP are ferromagnets at lower temperatures. The LTP after 240 h of milling exhibits a transition from the paramagnetic state to the spin-glass state upon cooling from room temperature, which is confirmed by some characteristic experiments. The representative results will be presented and discussed later in the paper. Apparently, the anomalies in the ac susceptibility vs temperature curves indeed correspond to the magnetic-ordering transition. The data shown in the third and/or fourth column in Table I are the ferromagnetic Curie temperatures T_C of the various samples and/or the freezing temperature T_f of the amorphous phase. The T_C values derived from the Arrott plots are given in Table II, which are in good agreement with those obtained from the corresponding ac susceptibility vs temperature curves as seen in Table I. The effective magnetic moment per Co atom in the LTP is slightly larger than that in the HTP, while it is much smaller than that of the LTP after 60 h and 240 h of milling. That the effective magnetic moment per Co atom of the LTP is also increased after mechanical milling means that the angular momentum of Co atoms increases during milling. This means that

TABLE II. The effective magnetic moment p_{eff} (μ_B/Co atom), paramagnetic Curie temperature θ_p (K), ferromagnetic Curie temperature T_C (K) or freezing temperature T_f (K) of the LTP after 0, 60, and 240 h of milling and the HTP. For direct comparison, the phase status is also listed. The values of T_C estimated from Arrott plots slightly deviate from those obtained from ac susceptibility vs temperature measurements.

Sample	p_{eff} (μ_B/Co atom)	θ_p (K)	T_C (K)	T_f (K)	Phase status
α-Co_2Ge (LTP)	1.29	56.3	47		Ordered crystalline
60 h	2.13	117.2	86		Disordered crystalline
240 h	2.66	61.7		43.1	Amorphous state
β-Co_2Ge (HTP)	1.26	20.0	6		Ordered crystalline

atomic disorder really takes place during milling leading to a change in the nearest neighbor configuration of a Co atom and in atomic distances. We now present some typical experimental results obtained on the amorphous phase (the LTP milled for 240 h).

Theoretically (see for instance Refs. 13 and 14 and references therein), the most characteristic features defining a spin-glass are the sharp cusp at the freezing temperature T_f in the temperature dependence of the ac susceptibility (χ) and the sensitive external-magnetic-field dependence of χ; the difference in value and shape between the magnetization vs temperature curves after zero-field cooling and after field cooling at the temperatures below T_f; the displacement of the magnetization curve with respect to the zero of the field and the corresponding unidirectional remanence at low temperatures after cooling in a magnetic field from above T_f to a much lower temperature. Figure 13(a) shows the temperature dependence of the real part of the ac susceptibility χ' of the amorphous phase (the LTP milled for 240 h) for different amplitudes of the external field. The temperature dependence of the imaginary part of the ac susceptibility χ'' of the sample is displayed in Fig. 13(b). The value of χ'' gives the energy absorption by the material. The intensity of the signals has been normalized using the value of the applied ac fields (ac currents). The frequency used for the measurement is 14.3 Hz. From Fig. 13(a) the following points can be clearly noticed. (i) A very sharp cusp is evident when the field used is very low but it is destroyed and becomes a broad maximum by an increase of the external field. When the applied field is increased to 0.015 T we can even not observe a maximum within the temperature range measured; (ii) the intensity of the cusp decreases with increasing amplitude of the applied field. (iii) The peak temperature decreases with increasing amplitude of the applied field. These phenomena are very similar to those observed by Bhagat *et al.*[15] in the amorphous spin-glass $(Fe,Ni)_{75}P_{16}B_6Al_3$ alloys and by Cannella and Mydosh in typical spin-glass AuFe alloys.[16] In addition, from Fig. 13(b) it is seen that the energy absorption by the sample increases with increasing amplitude of the applied field and that the temperature where χ'' reaches a minimum value shifts to lower temperature with increasing external fields. In a field of 0.015 T heating by eddy currents makes it impossible to measure to the lowest temperatures. Figure 14 shows the variation of the magnetization with temperature in the LTP after

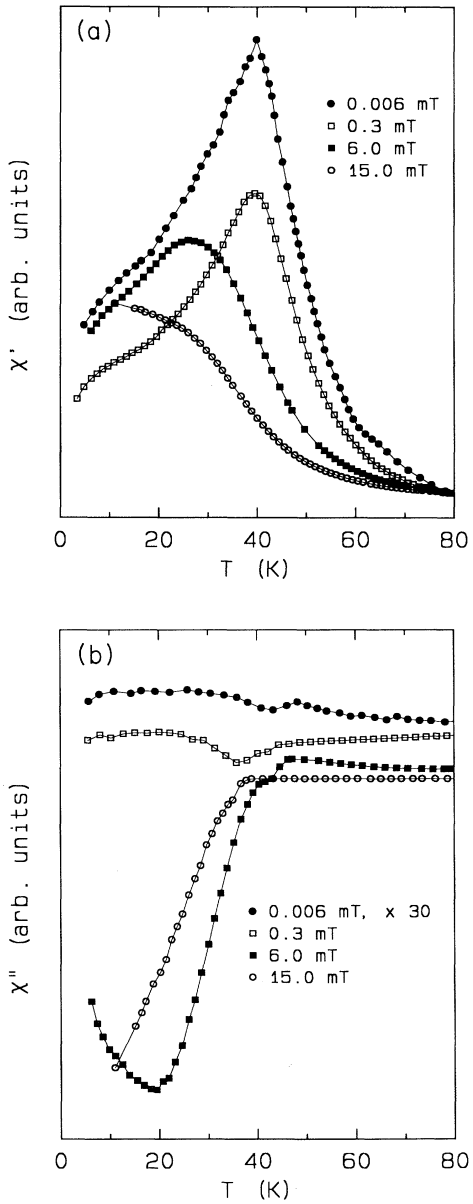

FIG. 13. Temperature dependence of the real part χ' (a) and the imaginary part χ'' (b) of the ac susceptibility of the LTP after 240 h of milling in the different amplitudes of the external ac field. The frequency of 14.3 Hz was used during measuring.

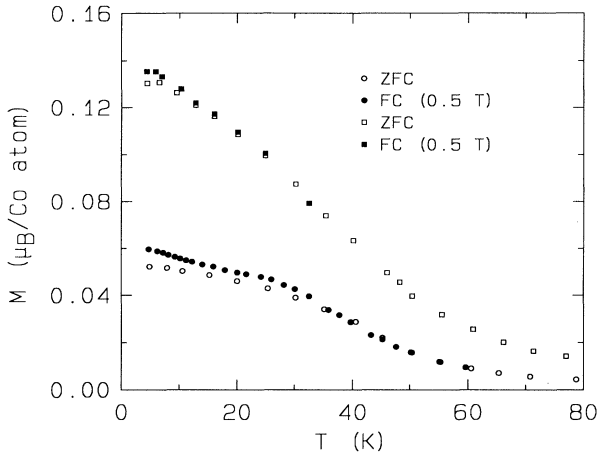

FIG. 14. Temperature dependence of the magnetization of LTP after 240 h of milling measured at 0.025 T (circles) and 0.1 T (squares). Open symbols denote zero-field cooling (ZFC) and filled symbols are field cooling (FC) in a field of 0.5 T.

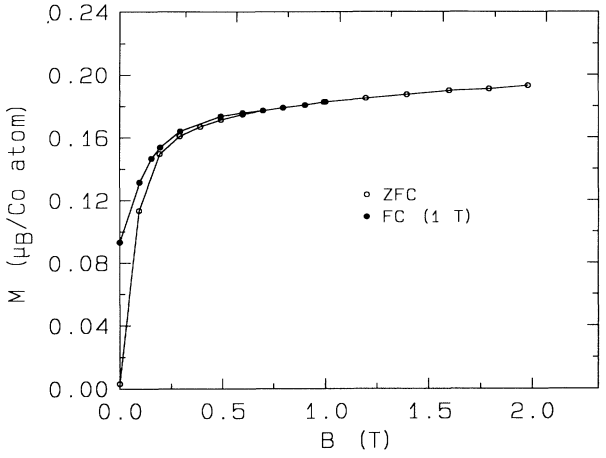

FIG. 15. Magnetization curves of the LTP after 240 h of milling with zero-field cooling (ZFC) and field cooling (FC) in a field of 1 T.

240 h of milling in two different applied magnetic fields of 0.025 and 0.1 T. After zero-field cooling (ZFC) and field cooling (FC) in a field of 0.5 T, the measurements were successively made during heating the sample. It is clear that in a certain magnetic field the values of the magnetization after ZFC and FC are different at temperatures below T_f. With increasing temperature the difference in magnetization decreases gradually. At temperatures around T_f and above, the two curves are found to coincide. With the increase of the applied field during measuring, T_f shifts to lower temperatures. The coincident temperature for the sample measured at 0.025 T is about 35 K and it decreases to about 15 K when the sample was measured in 0.1 T. We did not observe a maximum in the curve of the sample after zero-field cooling like in other spin glasses [see, for instance, Ref. 17 for the amorphous spin glass $(Co,Ni)_{75}P_{16}B_6Al_3$]. This is easily understood from the fact that the sharp cusp in the ac susceptibility vs temperature curves becomes a rounded transition when a field of a few Gauss is used and is completely destroyed by a field of 0.015 T. Due to the difficulty to obtain a very low dc field, the minimum dc field used here during the measurement is 0.025 T. This may be enough to conceal the fact that a maximum around the freezing temperature should be observed in the magnetization vs temperature curve for the spin-glass amorphous phase after ZFC. It was really shown in Ref. 17 that in the amorphous spin glass $(Co,Ni)_{75}P_{16}B_6Al_3$ a rounded maximum is observed in a field of 10 Oe and that this disappeared when the field is higher than 30 Oe. Figure 15 shows a displaced magnetization curve at 4.4 K for the LTP milled for 240 h after cooling in a field of 1 T (FC), together with the magnetization curve measured after cooling the same specimen in zero field (ZFC) to 4.4 K. The remanence is approximately $0.09\mu_B$/Co atom whereas there is no remanence in the specimen after zero-field cooling within experimental accuracy. The two curves are found to coincide at a field of 0.6 T. All together the results shown above prove that the amorphous phase obtained by mechanical milling of the LTP undergoes a paramagnetic to spin-glass (SG) transition at about 43 K (the freezing temperature, T_f) upon cooling from room temperature, rather than a paraferromagnetic transition. The freezing temperature shifts to lower temperature with increasing magnitude of the applied magnetic field.

B. Hexagonal β-Co_2Ge (HTP)

1. Structure and thermal stability

The above described investigation was originally undertaken in order to assess whether similar results would be obtained as in the analog systems Ni_3Sn_2 and Co_3Sn_2, which were studied previously. The latter compounds transformed from the LTP to the HTP during ball milling. However, it was experimentally found that such a transformation is not observed during mechanical milling of the α-Co_2Ge (LTP), which in contrast amorphizes. In an attempt to obtain amorphous Co_2Ge by melt spinning for comparison, we quenched this material from the liquid state to room temperature with a cooling rate of 10^7 K/s. It turned out that it is impossible to obtain the amorphous phase of this compound by the traditional melt-spinning technique. As can be seen from Fig. 16 (the pattern marked as 0 h) the material obtained by melt spinning is crystalline with Ni_2In-type hexagonal structure [characteristic of the high-temperature phase β-Co_2Ge (HTP)]. No amorphous fraction is detected. In order to assess whether the HTP would also become amorphous upon milling like the LTP we ball milled the HTP as well.

X-ray-diffraction patterns of the HTP after various periods of milling are shown in Fig. 16. It is seen that the pattern of the melt-spun sample (0 h) is the same as that of the sample quenched from 800 °C (see HTP in Fig. 2). It is clear that the intensity of all peaks of the HTP decreases sharply with increasing milling time. After 5.7 h

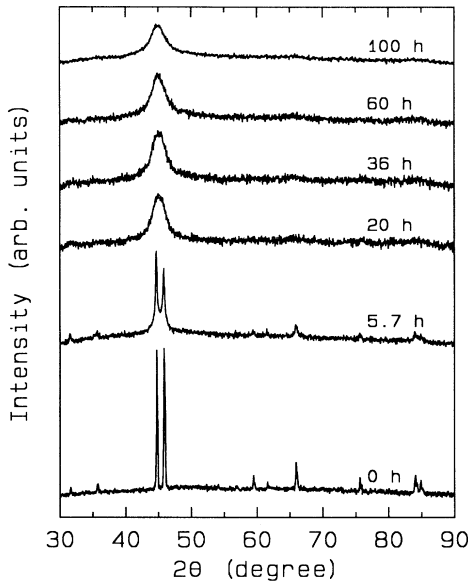

FIG. 16. X-ray-diffraction patterns of the HTP after various periods of milling.

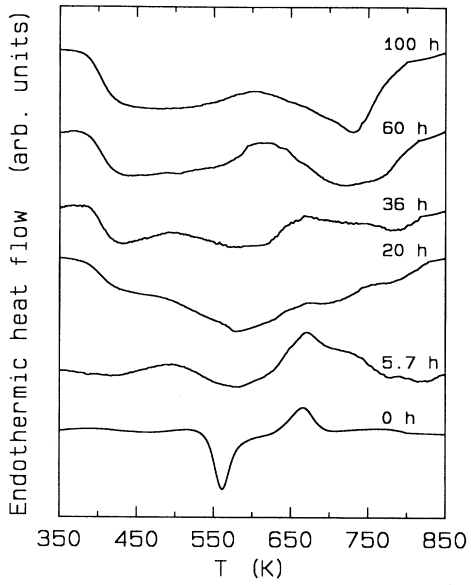

FIG. 17. DSC scans of the HTP after various periods of milling. The heating rate was 10 K/min.

of milling, some of the Bragg peaks disappear and the other peaks become rather broad compared with the pattern of the starting compound (0 h). After 20 h of milling, almost all peaks disappear except for a rather broad peak at $2\theta=45°$, which is characteristic of an amorphous phase. This means that the HTP becomes completely disordered and that the material is transforming to the amorphous state at a milling time of 20 h. After 36 h of milling, all the Bragg peaks disappear except for the broad halo at $2\theta=45°$. This means that the amorphization is completed after 36 h of milling. Hardly any changes occur in x-ray diffraction upon further milling. This means that there is no structural change in the late stage of milling. But, in fact the material is homogenized. This is found from the change of the sharpness of the cusp in magnetic susceptibility measurements (see Fig. 20).

The DSC scans of the HTP after various periods of milling are shown in Fig. 17. The behavior upon heating of the melt-spun HTP (0 h) is very similar to that of the HTP quenched from 800 °C. An exothermic transition is observed at 560 K which corresponds to the phase restoration of the metastable HTP to LTP. Upon further heating, an endothermic peak at 670 K is detected which is responsible for the equilibrium phase transition from LTP to HTP appearing in phase diagram. The transition temperature is somewhat lower than that in the LTP. Upon ball milling, the peak temperature of the endothermic transition shifts somewhat to lower temperature and the heat involved in the endothermic transition decreases with increasing milling time. After 5.7 h of milling, the exothermic peak becomes rather broad. This indicates another exothermic effect which results from the atomic reordering process. Additionally, a weak exothermic peak at 420 K is observed in the DSC scan which is due to the release of strain induced by the milling. After 20 h of milling, the exothermic peak at about 420 K (the first exothermic transition) becomes much more pronounced, which reflects the fact that there is another strong exothermic heat effect included in this peak, which corresponds to the crystallization of the amorphous phase. Meanwhile, another weak exothermic transition at about 780 K is observed which is responsible for the subsequent growth of the nanocrystallites. Upon further milling the first exothermic peak becomes more and more pronounced and finally reaches a constant heat content of about 4 kJ/mol in the temperature range from 380 to 580 K. This is close to the value of the heat involved in the same process of the amorphous phase obtained by ball milling of the LTP. In fact, this is the total heat involved in the crystallization and the subsequent atomic ordering.

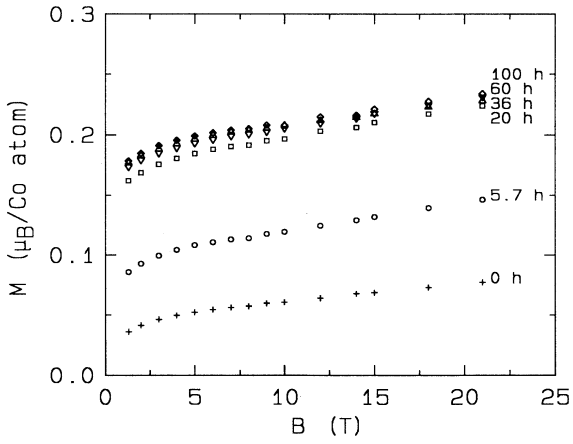

FIG. 18. High-field magnetization curves at 4.2 K of the HTP after various periods of milling.

TABLE III. Magnetic moment M (μ_B/Co atom) at 4.2 K, ferromagnetic Curie temperature T_C (K) or freezing temperature T_f (K), and the phase status of the HTP upon mechanical milling.

Milling time (h)	M (μ_B/Co atom)	T_C (K)	T_f (K)	Phase status
0 (β-Co_2Ge HTP)	0.077	5		Ordered crystalline
5.7	0.146	22.4		Disordered crystalline
20	0.224	33.8		Crystalline+amorphous
36	0.231		34.9	Amorphous
60	0.234		34.4	Amorphous
100	0.238		34.7	Amorphous

The peak temperature shifts somewhat to higher temperature upon milling. The endothermic peak shifts to 600 K and the heat involved in the transition is estimated as 0.2 K/mol. The last exothermic peak also becomes more pronounced upon further milling. The heat involved in the transition is estimated as 1.0 kJ/mol and the peak temperature shifts to 730 K in the sample milled for 100 h.

2. *Magnetic properties*

Figure 18 shows high-field magnetization curves at 4.2 K of the HTP after various periods of milling. The value of the magnetic moment per Co atom at 21 T is tabulated in Table III. It is clearly seen that the magnetization increases sharply with increasing milling time. After 36 h of milling it reaches a value of 0.231μ_B/Co atom. This is quite close to the value of the magnetization of the final product obtained by milling of the LTP. Upon further milling, the value of the magnetization only slightly increases with milling time. The magnetization curves of some typical samples measured at 77 K are displayed in Fig. 19. From this figure it is observed that in an external field the magnetization behavior at 77 K of the samples milled for 0 and 5.7 h is quite similar. However, the sample milled for 20 h behaves differently. This indicates that the latter sample is mainly a different magnetic phase which is amorphous.

The magnetic-ordering temperatures were obtained from the ac magnetic susceptibility vs temperature measurements. As a check, the measurement of the magnetization as a function of an external field at various temperatures was also performed on the sample after 5.7 h of milling. Figure 20 shows the temperature dependence of the real part of the ac magnetic susceptibility χ' of the HTP after various periods of milling. In the curve of the starting compound (0 h) an upturn at about 5 K is observed, which corresponds to the paraferromagnetic transition. After 5.7 h of milling it becomes a broad maximum at about 22 K. After 20 h of milling, the maximum shifts to higher temperature. After 36 h of milling, it becomes a sharp cusp at somewhat higher temperature. The transition temperatures derived from these curves using the same method as in Sec. III A 2 is collected in Table III. On further milling, the cusp becomes sharper and sharper and the cusp temperature is only slightly dependent on milling time. This means that the material becomes more and more homogeneous upon further milling. Figure 21 displays the Arrott plots of the HTP after 5.7 h of milling. The Curie temperature is that temperature for which the straight line goes through the origin. From this figure the Curie temperature T_C of the sample

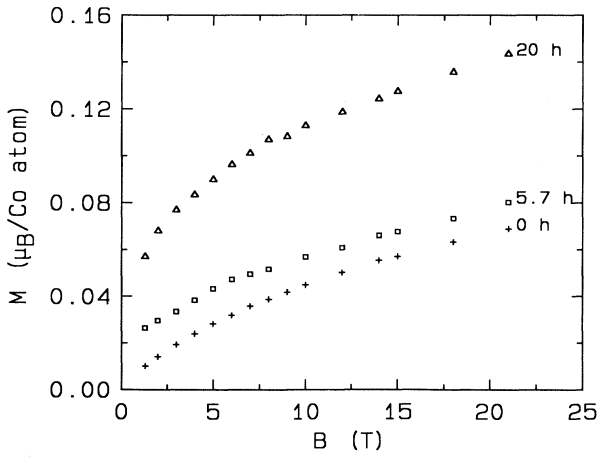

FIG. 19. High-field magnetization curves at 77 K of the HTP milled for 0, 5.7, and 20 h.

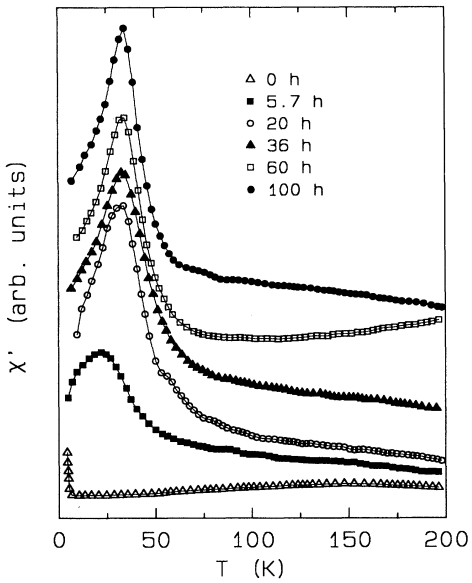

FIG. 20. Temperature dependence of the real part of the ac susceptibility χ' of the HTP after various periods of milling in an external ac field of 0.06 mT. The frequency of 109 Hz was used during measuring.

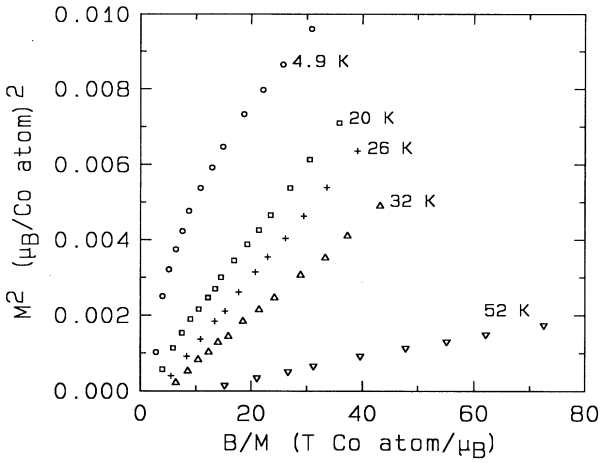

FIG. 21. The Arrott plots of the HTP after 5.7 h of milling.

can be estimated as about 23 K, which is close to the value obtained from the χ'' vs T curve.

IV. GENERAL DISCUSSION

The changes in magnetization and magnetic-ordering temperature of the intermetallic compounds α-Co_2Ge (LTP) and β-Co_2Ge (HTP) upon mechanical milling are consistent with the x-ray-diffraction patterns. That is, up to 60 h of milling for the LTP and up to 5.7 h for the HTP, the intermetallic compounds remain in the same structure as the starting compounds and the change in magnetization (M) and Curie temperature (T_C) is a continuous process. After milling for more than 180 h for the LTP and 36 h for the HTP the materials have transformed to an amorphous state and the value of the magnetization and of the magnetic-ordering temperature T_f is only slightly dependent on milling time.

The DSC scans together with the x-ray-diffraction results shown in Fig. 6 prove that the crystallization and the subsequent atomic ordering occur in the temperature range from 380 to 580 K accompanied by exothermic heat effects. That is, in the DSC scans in Fig. 4 for the LTP milled longer than 120 h and in Fig. 17 for the HTP milled longer than 20 h the first exothermic peak is responsible for the crystallization of the amorphous phase and the second exothermic transition corresponds to the subsequent atomic ordering process. The atomic reordering process in the disordered crystalline LTP and HTP is evident by the observation of a very broad exothermic transition. That is, the second exothermic peak in the DSC scans in Fig. 3 for the LTP milled shorter than 80 h and in Fig. 17 for the HTP milled shorter than 20 h is responsible for the atomic reordering of the disordered compounds to the ordered crystalline compounds.

The combination of the results of the x-ray diffraction, magnetic measurements, and DSC scans for the intermetallic compounds α-Co_2Ge (LTP) and β-Co_2Ge (HTP) after various milling times gives a clear picture of the mechanical milling process. The structure development of the LTP and the HTP during ball milling is summarized in the last column in Tables I and III, respectively. The process of mechanical milling of the LTP and the HTP can be divided into three stages.

The first stage is that the milling time is up to 60 h for the LTP and up to 5.7 h for the HTP. In this period, x-ray-diffraction patterns show that the materials remain in the same structure as the starting compounds (see Figs. 1 and 16), whereas the magnetization and Curie temperature continuously increase with milling time. The changes in magnetization and Curie temperature in both the LTP and the HTP upon mechanical milling could be understood in terms of atomic (chemical) disorder. In our previous investigations on an $A15$-structure superconducting compound,[18] a $B2$-structure magnetic compound[19] and a $B8$-structure *ferri*magnetic compound,[20] and a $B8$-structure *ferro*magnetic compound,[21] we were able to prove that atomic disorder was generated by mechanical milling. The type of atomic disorder turned out to be characteristic of the specific compound. According to Miedema's model,[24] the formation enthalpy of a binary-alloy system is mainly determined by the elastic energy and the chemical energy. If we neglect the relatively weak contribution of the chemical energy (compared to the elastic energy), from those investigations a conclusion could be drawn that if the atomic size of the different species of atoms in a fully occupied (no vacant lattice sites) crystalline structure is quite close, by mechanical milling antisite atomic disorder may be introduced in the material. In the crystal structure of the LTP and the HTP, cobalt atoms occupy two different types of lattice sites [octahedral (I) and tetrahedral (II) interstices], and both (I) and (II) sites are fully occupied. The LTP is very similar to the HTP, only the atoms are shifted somewhat from their positions to form an orthorhombic structure. Since the atomic size of metallic Co and Ge are almost of the same magnitude, it is very likely that antisite atomic disorder is generated in both the LTP and HTP under mechanical impact. This means that during mechanical milling Co and Ge atoms will exchange position. Such an exchange will lead to a variation of the neighborhood around a Co atom. From Fig. 8 we know that the average magnetic moment of cobalt atoms in the ordered crystalline state of LTP and HTP is approximately $0.1\mu_B$/Co atom, which is much less than $1.7\mu_B$/Co atom, the value for metallic cobalt.[22] The increase in magnetization can then be interpreted as follows: In the LTP and HTP germanium is a nonmagnetic element. This means that only the coordination of the Co atoms determines the formation of the magnetic moment in the intermetallic compounds. In the starting compounds, the Ge atoms surrounding a Co atom hinder the Co-Co interaction, which limits the formation of a large magnetic moment. During mechanical milling, due to the exchange of Co and Ge atoms, the neighborhood of a Co atom will also change. In this way clustering is favored with more and more Co atoms surrounding a Co atom. Such a Co-rich cluster will bear a larger magnetic moment because of an increasing probability of Co-Co exchange interaction. The number of the Co-rich clusters will gradually increase with increasing milling time. This will lead to an increase of the average magnetiza-

tion. Therefore, it is observed that in the first stage the magnetization of LTP and HTP continuously increases with increasing milling time.

The variation in Curie temperature of the LTP and HTP upon mechanical milling is due to the change of the magnetic moment of the cobalt atom. It is clearly seen from Tables I and III that the Curie point T_C of the LTP and the HTP increases continuously with increasing milling time. An increase in the Curie temperature in the process of milling is to be expected on the basis of the increased magnetic moment of these compounds. An increase in the probability of cobalt atoms appearing in the nearest neighborhood of a Co atom must raise the T_C, because the T_C value only depends on the Co-Co exchange interaction. The broadening of the transition in the ac susceptibility vs temperature curves, which transition is the ferroparamagnetic transition, is likely due to the size distribution of the Co-rich clusters. The size of the Co-rich clusters includes the number of the Co atoms and the relative distance between Co atoms in a Co-rich cluster. Due to the fact that the exchange of Co and Ge atoms is a continuous process during mechanical milling, it is likely that the number of the Co atoms and the relative distance between Co atoms in a Co-rich cluster are varying during milling. This means that there will be a distribution of the Co-rich cluster sizes during milling. Thus, the exchange integer, which determines the Curie temperature, will vary from cluster to cluster. This leads macroscopically to a broad transition in the ac susceptibility vs temperature curve as well as in the magnetization vs temperature curve.

Evidence for the atomic disorder is also obtained from the DSC analysis. The DSC scans clearly show that during heating of the materials after the first stage of milling a very pronounced exothermic heat effect is observed in the temperature range from 500 to 640 K, which corresponds to the atomic reordering process of the disordered compounds upon heating. The energy released in the process is about 3.3 kJ/mol.

The second stage of the mechanical milling takes place during the periods of more than 60 h and less than 180 h for the LTP, more than 5.7 h and less than 36 h for the HTP. In these periods the disorder drives amorphization. In fact the amorphization of the LTP starts at a milling time of 80 h, whereas it starts in the HTP somewhere between 5.7 and 20 h. In this stage, the x-ray-diffraction pattern becomes a broad halo. The magnetization further increases upon milling and finally becomes constant. More detailed information for understanding the process during this stage of milling can be obtained from the measurements of the ac susceptibility vs temperature. The appearance of an additional anomaly at 40 K after 80 h of milling strongly indicates the start of the amorphization. The coexistence of two anomalies in the LTP after 80 h milling means a mixture of crystalline material and the amorphous phase and gives evidence that the amorphization in the LTP is a continuous process. After 120 h of milling the anomaly at 40 K becomes predominant, which means that the majority of the material has been transformed to amorphous. After 180 h of milling the anomaly corresponding to the disordered crystalline material disappears and the anomaly of the amorphous phase becomes a pronounced cusp, which means that the material has completely transformed to the amorphous phase. The absence of the coexistence of two anomalies in the HTP during ball milling may be due to the fact that the time interval between 5.7 and 20 h is too long. After 20 h of milling of the HTP most of the material is transformed to amorphous.

Let us now discuss the DSC measurement results in this stage of milling. From Figs. 4 and 17 it is clear that the intensity of the first exothermic peak in the DSC scans increases with milling time. This also indicates the increase of the amorphous fraction with increasing milling time. Due to the fact that in this stage the material is a mixture of crystalline and amorphous materials, it is not possible to derive the heat involved in the process of the crystallization and the subsequent atomic ordering. In the following we will focus our discussion on the LTP milled for 180 h and the HTP milled for 36 h, in which the material is a single amorphous phase. The DSC scans clearly show a pronounced exothermic heat effect in the temperature range from 380 to 580 K, which corresponds to the crystallization of the amorphous phase and subsequent atomic ordering. This gives evidence that the crystalline material after crystallization is still atomically disordered. The total heat involved in the transition is about 4.2 kJ/mol for the LTP milled for 180 h and 4.0 kJ/mol for the HTP milled for 36 h. Since only a few peaks in the x-ray-diffraction pattern are observed, it is difficult to identify the structure of the material after crystallization. Upon heating both the LTP milled for 180 h and the HTP milled for 36 h undergo an equilibrium phase transition to the HTP accompanied by an endothermic heat effect. The heat involved in the endothermic (LTP to HTP) transition is estimated as 0.2 kJ/mol for both the LTP milled for 180 h and the HTP milled for 36 h. This is only 10% of the heat consumed for the ordered LTP and HTP during the same transition. This means that there are many defects introduced by mechanical milling such as antisite atoms and antiphase boundaries. Moreover, the crystalline materials obtained by the crystallization of the amorphous phase are nanocrystalline. This can be proved by the observation of the pronounced exothermic transition at about 740 K, which is dependent on milling time. It is also clear from Figs. 4 and 17 that the crystallization temperature shifts somewhat to higher temperature with increasing milling time, whereas the peak temperature of the exothermic transition corresponding to the growth of the crystallites shifts somewhat to lower temperature. This means that the amorphous fraction increases with increasing milling time as was discussed in Ref. 23. Therefore, we can claim that the increase of the crystallization temperature with increasing milling time is due to the increase of the amorphous fraction. In fact, the higher the amount of amorphous phase, the finer the crystallites after the crystallization are. The finer the crystallites, the higher the energy stored in grain boundaries is. Thus, the peak temperature for the growth of the nanocrystallites decreases with increasing milling time.

The third stage of milling is for periods longer than

180 h for the LTP and than 36 h for the HTP. In these periods the amorphization is completed and the material becomes homogeneous. All parameters and physical properties tend to become constant. The ferromagnetic moment at 4.2 K and effective magnetic moment of the amorphous phase are about $0.24\mu_B$ and $2.66\mu_B$ per Co atom, respectively. These are larger than twice the values in the original crystalline compounds.

Moreover, the amorphous phase is found to exhibit a transition at 43 K (freezing temperature, T_f) from the paramagnetic state to the spin-glass state upon cooling from room temperature to lower temperatures. This means that the spins in the amorphous phase are frozen in random directions at and below the freezing temperature. The freezing temperature decreases with increasing external magnetic fields due to the increase of the irreversible magnetization. To our best knowledge, this is the first time, that the amorphous phase synthesized by mechanical milling of an intermetallic compound shows spin-glass behavior. It appears that ball milling, which is a seemingly crude and rough technique, can generate a well-defined amorphous state having special properties. The peculiarity of the compound Co_2Ge is that the amorphous phase can not be obtained by traditional melt spinning. Mechanical milling offers a unique technique to obtain the amorphous phase of this compound. Why the amorphous phase of this compound can be obtained by ball milling but not by rapid quenching from the liquid is not clear. A possible reason might be that the amorphous phase of Co_2Ge produced by high-energy ball milling is more chemically disordered than the liquid. So the amorphous phase would not be formable from the liquid even at the highest quenching rates.

It is clear from all the experimental results that there is no evidence for a phase transformation from the orthorhombic structure α-Co_2Ge (LTP) to the hexagonal structure β-Co_2Ge (HTP) like in the similar systems Ni_3Sn_2 (Ref. 7) and Co_3Sn_2 (Ref. 8). Instead, a phase transformation from crystalline to amorphous is evident during mechanical milling of both the LTP and the HTP. This can be understood by inspecting the difference in crystal structure between Co_2Ge (LTP and HTP) on the one hand and Ni_3Sn_2 and Co_3Sn_2 on the other hand. All lattice sites are fully occupied in the Co_2Ge, whereas in the Ni_3Sn_2 and Co_3Sn_2 the lattice sites for the transition-metal atoms are only $\frac{3}{4}$ occupied. As mentioned before, in $B8$-like compounds the transition-metal atoms can occupy two different lattice sites (I and II). In the Ni_3Sn_2 and Co_3Sn_2, the position I is fully occupied whereas the position II is only half-occupied. On the other hand, the atomic radius of the Sn atom is much larger than that of the transition-metal atoms, whereas the atomic radius of a Ge atom is almost the same as that of a Co atom. Therefore, in Ni_3Sn_2 and Co_3Sn_2, it is more likely that during mechanical milling the transition-metal atoms redistribute over I and II sites. Such a redistribution will not destroy the structural frame at all because there is no exchange between transition-metal atoms and non-transition-metal atoms. However, in the Co_2Ge compounds, there is no such possibility for the redistribution of Co atoms on transition-metal sites, simply because all Co sites are occupied. All the results, shown above, prove that Co_2Ge disorders atomically in the early stage of milling. The only possible way for the atomic disorder is antisite disorder. Such antisite disorder destroys the original structure. Due to the exchange between Co atoms and Ge atoms the original structural frame is violated after long-time milling. Therefore, a phase transformation from the LTP to HTP during mechanical milling of LTP was not observed. The random distribution of different species of atoms and the refinement of the materials finally induce amorphization. In contrast, the energy stored in Ni_3Sn_2 and Co_3Sn_2 by the redistribution of transition-metal atoms during milling may be not high enough to reach the free energy level of the amorphous phase or solid solution of these compounds.

We will now discuss why Co_2Ge (LTP and HTP) finally transforms to an amorphous phase rather than to a solid solution. From calculations based on the Miedema semi-imperial model,[24] it turns out that the formation enthalpy of the amorphous state is slightly lower than that of the solid solution for this composition. So it is expected on the basis of Miedema's model that disordering would lead to the amorphous phase rather than to the crystalline solid solution. Therefore, the materials finally transform to the amorphous state.

All physical parameters of the final product obtained by mechanical milling of the LTP are quite close to those of the material obtained by ball milling of the HTP. Thus the final state obtained by mechanical milling of the LTP and the HTP is the same. The slight difference in the value of the freezing temperature may be due to a slight deviation of the composition of the sample during the melt-spinning process. This can be proved by the fact that the value of the Curie temperature and the magnetization of the HTP obtained by melt spinning is slightly smaller than that of the HTP obtained by quenching from 800 °C.

V. CONCLUSIONS

Both the low-temperature phase α-Co_2Ge (LTP) and the high-temperature phase β-Co_2Ge (HTP) are ferromagnetic at lower temperatures with a ferromagnetic Curie temperature T_C, of 46.4 and 6 K, respectively. The magnetic moment per Co atom at 4.2 K is $0.113\mu_B$ in the LTP and $0.103\mu_B$ in the HTP. The effective magnetic moment per Co atom is $1.29\mu_B$ in the LTP and $1.26\mu_B$ in the HTP.

Starting from both the ordered low-temperature phase α-Co_2Ge (LTP) and the ordered high-temperature phase β-Co_2Ge (HTP), mechanical milling generates atomic disorder in the early stage and finally transforms the materials to the amorphous phase. The process of mechanical milling can be divided into three steps. The first step is the disordering process of the LTP and the HTP. In this step, the x-ray-diffraction patterns of the milled samples reveal the same structure as the original compounds. The ferromagnetic moment at 4.2 K (M) and the Curie temperature (T_C) of the LTP and the HTP increase continuously with increasing milling time. The continuous

variation of M and T_C of the LTP as well as of the HTP gives evidence for atomic (chemical) disorder induced by mechanical milling. Antisite atomic disorder is proposed according to the increase of magnetization and Curie temperature of the LTP and the HTP with milling time. The exothermic transition in DSC scans corresponds to the atomic reordering process. The heat involved in the reordering process is about 3.3 kJ/mol. The second step is that the materials undergo a mechanically induced amorphization from the disordered LTP and HTP. In this stage, x-ray-diffraction patterns show a broad halo and the magnetization further increases and reaches a constant value upon further milling. The amorphization is a continuous process as can be seen from the ac susceptibility vs temperature measurements. That is, a mixture of two phases is detected by two anomalies in the ac susceptibility vs temperature curves. The appearance of the pronounced cusp and the disappearance of the transition corresponding to the crystalline phase strongly indicate the completion of the amorphization. The exothermic transition corresponding to the crystallization and the subsequent atomic ordering is evident. The heat involved in the process is approximately 4 kJ/mol. The last step is the completion of amorphization and the homogenization. In this period, all physical parameters tend to become constant. The effective magnetic moment and the magnetization at 4.2 K per Co atom in the amorphous phase are about $2.66\mu_B$ and $0.24\mu_B$, respectively. These are larger than twice the values in the originally ordered compounds. The amorphous phase exhibits a transition at about 43 K (freezing temperature, T_f) from the paramagnetic state to the spin-glass state upon cooling from room temperature to lower temperature. The magnetic properties show thermal hysteresis and relaxation below the spin-glass transition. The cusp in the ac susceptibility vs temperature curve becomes unsharp and T_f shifts to lower temperatures with increasing magnitude of the applied magnetic field.

The excellent agreement of all the results obtained by different techniques proves that by mechanical milling of the intermetallic compound Co_2Ge (LTP and HTP), well-defined nonequilibrium states are generated in the material. Apparently, a phase transformation from the orthorhombic structure LTP to the hexagonal structure HTP like in the similar systems Ni_3Sn_2 and Co_3Sn_2 is not observed. Instead, amorphization occurs during ball milling of both the LTP and the HTP. Together with the results obtained earlier on Ni_3Sn_2 and Co_3Sn_2 a general conclusion is that atomic disorder is the main source of the energy storage during milling of an intermetallic compound. The type of atomic disorder is characteristic of the specific compound and determines whether the materials transform to an amorphous state or to a solid solution. Antisite atomic disorder could be the condition for amorphization of an intermetallic compound by ball milling. Moreover, the measurement of magnetic properties is an important tool for monitoring the structural development of intermetallic compounds during mechanical milling. In particular, in case there is no significant change in x-ray-diffraction patterns and DSC traces in the intermediate stage of milling, it can provide detailed and precise information about the structural change of the compounds during milling.

ACKNOWLEDGMENTS

The authors are indebted to Professor P. F. de Châtel, Professor F. R. de Boer, and Professor V. Sechovsky for fruitful discussions. We would like to thank Dr. N. H. van Dijk and Dr. E. H. Brück for valuable discussions and useful suggestions. We thank Dr. V. H. M. Duijn and Dr. F. Kayzel for help with low-field magnetization measurements; H. Schlatter and Dr. D. M. R. Lo Cascio for help with quenching; A. C. Moleman and W. F. Moolhuyzen for help with x-ray diffraction. We gratefully acknowledge the Dutch Foundation for Fundamental Research on Matter (FOM) for financial support.

[1]A. Y. Yermakov, Y. Y. Yurchikov, and V. A. Barinov, Fiz. Met. Metalloved. **52**, 1184 (1981) [Phys. Met. Metallogr. (USSR) **52**, 50 (1981)].

[2]A. Y. Yermakov, V. A. Barinov, and Y. Y. Yurchikov, Fiz. Met. Metalloved. **54**, 935 (1982) [Phys. Met. Metallogr. (USSR) **54**, 90 (1982)].

[3]R. B. Schwarz and C. C. Koch, Appl. Phys. Lett. **49**, 146 (1986).

[4]A. W. Weeber, H. Bakker, and F. R. de Boer, Europhys. Lett. **2**, 445 (1986).

[5]H. Bakker and L. M. Di, Mater. Sci. Forum **88-90**, 27 (1992).

[6]T. Fukunga, M. Mori, M. Misawa, and U. Mizutani, Mater. Sci. Forum **88-90**, 663 (1992).

[7]G. F. Zhou, L. M. Di, and H. Bakker, J. Appl. Phys. **73**, 1521 (1993).

[8]L. M. Di, G. F. Zhou, and H. Bakker, Phys. Rev. B **47**, 4890 (1993).

[9]T. B. Massalski, in *Binary Alloy Phase Diagrams* (American Society for Metals, Metals Park, OH, 1986), p. 768.

[10]A. J. Riemersma, R. J. D. Manuputy, H. Schlatter, W. F. Moolhuyzen, R. Rik, D. M. R. Lo Cascio, and P. I. Loeff, Rev. Sci. Instrum. **62**, 1084 (1991).

[11]R. Gersdorf, F. R. de Boer, J. C. Wolfrat, F. A. Muller, and L. W. Roeland, in *High-Field Magnetism,* edited by M. Date (North-Holland, Amsterdam, 1983), p. 277.

[12]P. Villars and L. D. Calvert, in *Pearson's Handbook of Crystallographic Data for Intermetallic Phases* (American Society for Metals, Metals Park, OH, 1986), p. 1771.

[13]J. A. Mydosh, in *Ferromagnetic Materials,* edited by E. P. Wohlfarth (North-Holland, Amsterdam, 1980), Vol. 1, p. 71.

[14]P. A. Beck, Prog. Mater. Sci. **23**, 1 (1978).

[15]S. M. Bhagat, J. A. Geohegan, M. L. Spano, and H. S. Chen, J. Appl. Phys. **52**, 1741 (1981).

[16]V. Cannella and J. A. Mydosh, Phys. Rev. B **6**, 4220 (1972).

[17]Y. Yeshurun, K. V. Rao, M. B. Salamon, and H. S. Chen, J. Appl. Phys. **52**, 1747 (1981).

[18]L. M. Di, P. I. Loeff, and H. Bakker, J. Less-Common Met. **168**, 183 (1991).
[19]L. M. Di, H. Bakker, Y. Tamminga, and F. R. de Boer, Phys. Rev. B **44**, 2444 (1991).
[20]G. F. Zhou and H. Bakker, Phys. Rev. B **48**, 7672 (1993).
[21]G. F. Zhou and H. Bakker, in *Mechanical Alloying for Structural Applications,* edited by J. J. de Barbadillo (American Society for Metals, Metals Park, OH, in press); and (unpublished).
[22]E. P. Wohlfarth, in *Ferromagnetic Materials,* edited by E. P. Wohlfarth (North-Holland, Amsterdam, 1980), Vol. 1, p. 1.
[23]L. C. Chen and F. Spaepen, Mater. Sci. Eng. A **133**, 342 (1991).
[24]H. Yang and H. Bakker, J. Alloys Compounds **189**, 113 (1992), and the internal book.